Suppression of ferromagnetic order in CuO/Cu_2O nanocomposites

R. Das[1,2,*], J. Alonso[3], E. M. Jefremovas[3], L. Fernández Barquín[3], P. K. Ngoc[1,2], H. T. Nguyen[2,4], D. T. Viet[5], P. V. Vinh[6], A. T. Duong[1,2]

[1]*Faculty of Materials Science and Engineering, Phenikaa University, Hanoi 12116, Vietnam*

[2]*Phenikaa Research and Technology Institute (PRATI), A&A Green Phoenix Group, 167 Hoang Ngan, Hanoi 13313, Vietnam*

[3]*Departamento CITIMAC, Universidad de Cantabria, Santander 39005, Spain*

[4]*Faculty of Electrical and Electronic Engineering, Phenikaa University, Hanoi, 12116, Viet Nam*

[5]*Academy of military science and technology, 17 Hoang Sam, Cau Giay, Hanoi 10000, Vietnam*

[6]*Faculty of Physics, Hanoi National University of Education, 136 Xuan Thuy, Cau Giay, Hanoi, Vietnam*

Corresponding author: raja@phenikaa-uni.edu.vn

Abstract: 11 nm diameter quasi-spherical and single phase CuO/Cu_2O nanocomposites, with varying CuO:Cu_2O ratio, were synthesized using solvothermal process. X-ray diffraction patterns refined with the Rietveld method show an evolution of the CuO:Cu_2O ratio (%) for the three samples (100:0, 66:34, and 9:91), along with an increased lattice deformation of the CuO unit cell as the amount of Cu_2O increased: a = 4.653(2) Å, b = 3.411(1) Å, and c = 5.131(1) Å for the single phase CuO nanoparticles, similar to bulk, while a = 4.727(2) Å, b = 3.457(3) Å, and c = 5.247(2) Å for the 9/91 % CuO/Cu_2O nanocomposites. Magnetic measurements as a function of the temperature (M vs T) and as a function of the magnetic field (M vs H) nanoparticles indicated the presence of a ferromagnetic phase in the whole range of temperatures for the single phase CuO nanoparticles, as revealed by the persistent hysteresis observed in the M vs H loops. In addition, an enhanced antiferromagnetic contribution, denoted by the increase in the antiferromagnetic susceptibility, χ_{AF}~ 4.8 10^{-6} emu·g^{-1}·Oe^{-1}, is also observed for these single phase CuO nanoparticles, while for bulk CuO, χ_{AF} ~ 0.6 10^{-6} emu·g^{-1}·Oe^{-1}. With increasing Cu_2O content (≥ 34 % Cu_2O), the ferromagnetic phase is drastically suppressed for all temperatures, whereas the antiferromagnetic contribution at low temperatures (2-5 K) first increases (χ_{AF} ~ 5.1 10^{-6} emu·g^{-1}·Oe^{-1} for 34 % Cu_2O), but then, it gets reduced (χ_{AF} ~ 1.46 10^{-6} emu·g^{-1}·Oe^{-1} for 91 % Cu_2O). These magnetic changes showcase the relevance of the interface effects introduced by the Cu_2O phase in CuO/Cu_2O nanocomposites.

Introduction

The study of the magnetic properties of antiferromagnetic (AF) nanoparticles compared to their bulk form has become an active area of research due to the novel phenomena arising at the nanoscale [1–6]. Most of the works in this field have been focused on transition metal mono oxides [4,6,7]. To this respect, CuO and Cu_2O occupy a special place among these materials due to their unique structure and physical properties. CuO and Cu_2O are p-type semiconductors with a narrow band gap, and have attracted great attention due to the potential industrial applications, such as catalysis, gas sensing, magnetic storage, solar energy conversion, plastics, paints, etc. [7–14]. The magnetism of bulk CuO is already interesting, because of the square-planar coordination of copper by oxygen, which resembles high-T_C superconductors. Furthermore, CuO undergoes a paramagnetic to incommensurate antiferromagnetic transition at 230 K, followed by a first order transition from an incommensurate to a commensurate antiferromagnetic state at 213 K [15–22]. When the size of CuO is reduced to the nanoscale, the uncompensated surface magnetic moments dominate the magnetic behavior of these nanoparticles, due to the lower coordination and uncompensated exchange coupling of the surface atoms, resulting in a considerable change of the magnetic properties [23]. For example, Punnoose *et al.* [7] reported a decrease of Néel temperature when the size of CuO nanoparticles got reduced. Apart from this, weak room temperature ferromagnetism (FM) has also been reported in CuO nanoparticles with sizes below 10 nm [7,8] The reason for this FM behavior is not entirely clear, and it has been related to several possible origins, such as oxygen vacancies, change in spin arrangement, point defects, impurities, and dislocations, among others [23–29]. On the other hand, when the stoichiometry in Cu:O is changed from 1:1 to 2:1, the magnetic ordering is lost. Unlike CuO, bulk Cu_2O is diamagnetic: neither Cu^{+1} nor O^{-2} are magnetic ions, since the *d* shell of Cu^{+1} is full [30]. Nevertheless, surprisingly, the size

reduction to the nanoscale seems to endow the Cu_2O nanoparticles with a magnetically ordered state, where some form of room temperature ferromagnetism has been reported [30,31].

A further step in this research area consists in studying CuO/Cu_2O composites. To this respect, there have been a few works on the magnetic properties of CuO/Cu_2O in bulk and microspheres [32,33], but studies on the magnetic properties of CuO/Cu_2O nanocomposites are missing. For example, Gao *et al*. [32] reported the appearance of room temperature FM in CuO/Cu_2O microspheres. The room temperature FM initially became stronger with the increase of the Cu_2O phase up to 27% content, but it rapidly decreased when the Cu_2O phase increased above 90%. The appearance of this FM behavior was in principle associated to an indirect exchange coupling at the interface between the 2 phases, though further work is needed to shed light on this issue. Considering all this, it is clear that tailoring the interface in CuO/Cu_2O can open the door to enhanced magnetic properties and emergent phenomena in these materials, which could be interesting for different applications, such as spintronics [33].

To further investigate the effect of the size reduction on the magnetic properties of these transition metal oxides, in this work, 11-12 nm CuO/Cu_2O nanocomposites have been synthesized with varying $CuO:Cu_2O$ ratio (%): 100:0 (sample S1), 66:34 (sample S2), and 9:91 (sample S3). The structure and magnetic properties of these samples have been analyzed using X-ray diffraction (XRD) measurements with Rietveld refinement, Transmission Electron Microscopy (TEM), and a combination of magnetic measurements: magnetization vs. temperature (M vs. T), and magnetization vs. magnetic field (M vs. H). The obtained results reveal the presence of a FM phase in single phase CuO nanoparticles for the whole range of temperatures, while with increasing Cu_2O content, the FM phase is drastically suppressed. In addition, with increasing Cu_2O content, the AF

contribution first appreciably increases for 34 % Cu_2O, as compared to bulk, but then, it gets reduced for 91 % Cu_2O.

Experimental Methods

Synthesis of CuO and CuO/Cu_2O composites

The CuO (S1) and CuO/Cu_2O (S2 and S3) nanocomposites used in the present study were synthesized by the solvothermal process. In a typical synthesis, $Cu(CH_3COO)_2 \cdot H_2O$ was dissolved in 35 ml ethanol and kept for 15 min under magnetic stirring. Then the precursor solution was transferred to a 45 ml Teflon-lined autoclave and kept at desired temperature for 24 h. The autoclave was cooled to room temperature naturally and the precipitate was washed with ethanol three times to remove unreacted precursors. The resulting sample was dried at room temperature in air. The reaction temperature (130-150 °C) was varied to obtain CuO/Cu_2O nanocomposites with different CuO:Cu_2O ratio: 100:0 (130ºC, sample S1), 66:34 (140ºC, sample S2), and 9:91 (150ºC, sample S3).

Characterization of the samples

X-ray Diffraction analysis (XRD) was carried out using a Bruker AXS D8 X-ray diffractometer working in Bragg–Brentano geometry with Cu-Kα (λ = 1.5418 Å) radiation. The obtained XRD patterns were analyzed using Rietveld refinement. For the preparation of the samples, several drops of each sample were casted onto a piece of a Si wafer, and left to dry until a homogeneous layer was obtained. The measurements were carried out between 20 and 80º, with a step of 0.05º.

Transmission electron microscopy images were obtained using a FEI Morgagni 268 Transmission Electron Microscope (TEM) operating at 60 kV. For the preparation, the samples were diluted in

hexane and sonicated for a few minutes. Afterward, one drop of each sample was casted onto a Cu grid and inserted inside the TEM instrument for imaging.

Magnetic measurements were done using a Quantum Design Physical Property Measurement System (PPMS) with the vibrating sample magnetometer (VSM) option. All the magnetic measurements were carried out with the samples in powder form inside a gel capsule. *M* vs. *T* curves were recorded between 5 and 350 K following the zero-field-cooling/field-cooling (ZFC/FC) protocol. During the ZFC, the sample was cooled in the absence of magnetic field down to 5 K, then a magnetic field (100 or 500 Oe) is applied, and the magnetization was measured while increasing the temperature. On the other hand, during FC, the sample was cooled in the presence of the same magnetic field, and then the magnetization was recorded with increasing temperature, while keeping the field applied. On the other hand, *M* vs. *H* loops were measured at 2, 5, and 300 K, applying fields up to 50 kOe. For the exchange bias analysis, a magnetic field of 50 kOe was applied at 300 K and the sample was cooled down to 5 K in the presence of this field. Afterwards, the *M* vs. *H* was recorded at this temperature.

Results and discussion

The structural phases of the samples were determined using powder X-ray diffraction (XRD). XRD patterns of the CuO and CuO/Cu_2O composites nanoparticles are shown in **Figure 1** along with the corresponding Rietveld refinements (see **Table I** for the refined parameters).

As depicted, the XRD patterns corresponding to sample S1 confirm a single monoclinic CuO phase (space group symmetry *C 2/c*). The corresponding lattice parameters, a = 4.653(2) Å, b = 3.411(1) Å, and c = 5.131(1) Å, are similar to those reported in bulk CuO, a_{bulk} = 4.653(10) Å, b_{bulk} = 3.410(10) Å, and c_{bulk} = 5.108(10) Å [34]. Contrary to other studies in similar CuO nanoparticles,

no increase in the *b* axis was observed for sample S1 [7]. The performed refinements also indicate the existence of a preferred orientation along the (111) direction. The low Bragg factor obtained, R_B = 7.2 %, ensures the reliability of the fittings. Rietveld refinements also provide information on the nanocrystalline size, <*D*>, and microstrain, η. For S1, <*D*> = 10.6(1) nm and η = 0.15%, indicating a low microstrain, with a slight modification of the β angle, which reaches a value of 98.94(5)º for S1, slightly smaller than the bulk value, β_{bulk} = 99.53(4)º.

Rietveld refinements performed on sample S2 clearly reveal the coexistence of both CuO (66%) and Cu_2O phases (34%). The former CuO phase keeps the same monoclinic arrangement as in S1, with unit cell values *a* = 4.694(2) Å, *b* = 3.425(2) Å and *c* = 5.173(1) Å and β = 99.09(4)º, indicating a slight unit cell expansion with respect to S1. This relaxation of the unit cell goes along with a larger microstrain, η = 0.28(4)% for S2. Regarding the Cu_2O phase, the Rietveld refinements indicate a cubic Cu_2O-type structure (*Pn-3n*) (cuprite), being the obtained lattice parameter *a* = 4.269(3) Å. This value is in very good agreement with the one reported for bulk Cu_2O (*a* = 4.2696 Å) [35]. Finally, the mean nanoparticle size for S2 is <*D*> = 10.4(3), and the Bragg factors are R_B = 6.8 % and R_B = 9.7 % for CuO and Cu_2O phases, respectively.

In the case of sample S3, XRD data indicate that amount of CuO phase greatly decreases, as the obtained phase content are 9% and 91% for the CuO and Cu_2O phases, respectively. In this case, the CuO phase also arranges in a monoclinic structure, with *a* = 4.727(2) Å, *b* = 3.457(3) Å and *c* = 5.247(2) Å, and β = 97.5(4)º, yet the structure is even more distorted than before, being η = 0.52 (2)%. Indeed, the increase of the Cu_2O content alters the crystalline structure of the monoclinic CuO phase. The Cu_2O phase, on the other hand, exhibits the already mentioned cubic structure (*Pn-3n*), with a lattice parameter *a* = 4.2757(2) Å. Rietveld refinements inidcated a mean

nanoparticle size of <*D*> = 10.5(3) nm for sample S3, and Bragg factors in this case are R_B = 11 % and R_B = 2 % for CuO and Cu_2O phases, respectively.

All in all, XRD and Rietveld analysis indicate that the 3 samples have a very similar nanocrystalline size, and, while the pure CuO nanoparticles present lattice parameters similar to te bulk CuO, as the Cu_2O content increases, a progressive distortion of the CuO unit cell is clearly observed in the CuO/Cu_2O nanocomposites.

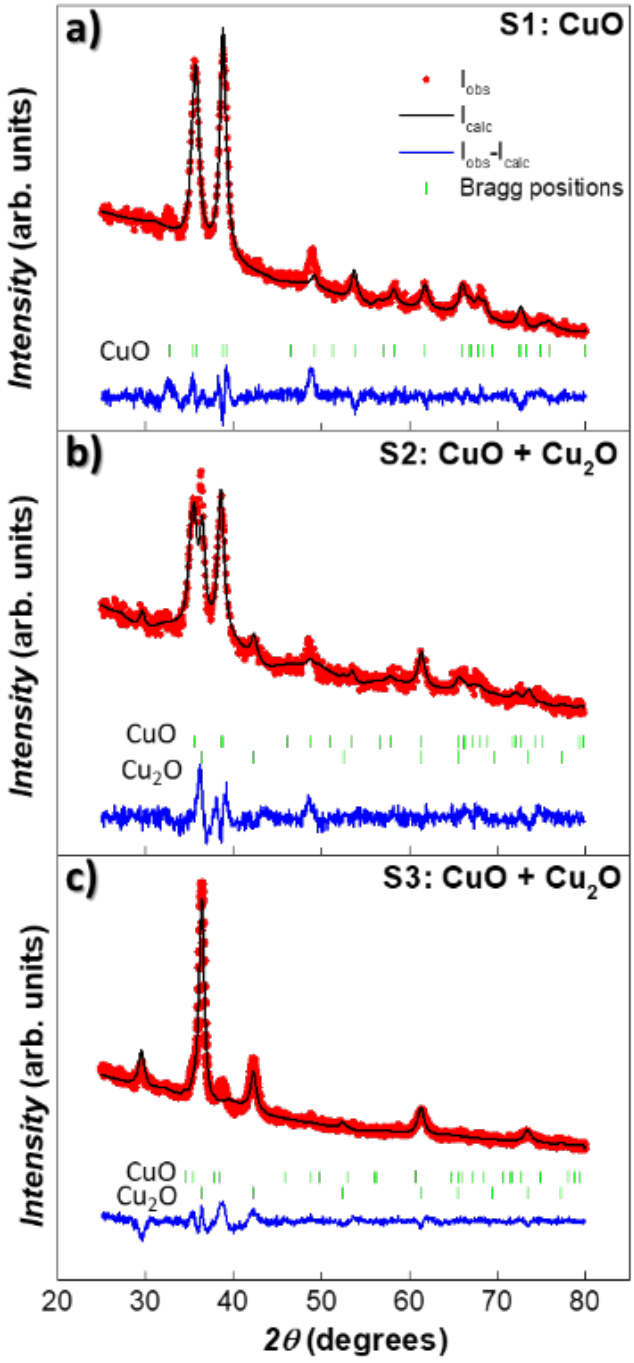

Figure 1. X-ray diffraction patterns corresponding to samples a) S1, b) S2 and c) S3. Red dots represent the experimental data, the black line accounts for the calculated Rietveld refinements, being the bottom blue line the difference between the experimental (I_{obs}) and the calculated (I_{calc}) profiles. Green vertical bars correspond to the CuO (top) and Cu_2O (bottom) hkl reflections.

Table I. CuO/Cu_2O ratio, crystallite size <*D*> (XRD), average size obtained by TEM (D_{TEM}), standard deviation (σ_{TEM}), and lattice parameters for CuO (*a, b, c*) and Cu_2O (*a*).

Sample	CuO/Cu_2O ratio (%)	<*D*> (nm)	D_{TEM} (σ_{TEM}) (nm)	*a* (Å) CuO	*b* (Å) CuO	*c* (Å) CuO	*a* (Å) Cu_2O
S1	100/0	10.6(1)	11 (2)	4.653(2)	3.411(1)	5.131(1)	-
S2	66/34	10.4(3)	11 (2)	4.694(2)	3.425(2)	5.173(1)	4.269(3)
S3	9/91	10.5(3)	12 (2)	4.727(2)	3.457(3)	5.247(2)	4.2757(2)

The morphology and particles size of CuO/Cu_2O nanocomposites were analyzed using Transmission Electron Microscopy (TEM). **Figure 2** shows TEM images of the nanoparticles along with their particle size distribution. The mean diameter, D_{TEM}, and standard deviation, σ_{TEM}, are presented in **Table I**. The TEM images illustrate the formation of quasi-spherical particles, with a relatively narrow size distribution, but very agglomerated, as can be observed in the inset to **Figure 2**. **Figure 2a** reveals that the CuO nanoparticles (S1) have a mean diameter D_{TEM} = 11 nm, with a standard deviation σ_{TEM} = 2 nm, as deduced from fitting the size distribution histograms to a Log-Normal distribution. These values are close to the ones estimated by XRD. These TEM images also show that the average particle size does not change appreciably with increasing Cu_2O content (S2 and S3), as depicted by the histograms presented in **Figures 2d-f**. TEM results also reveal that the 3 samples exhibit similar morphology and size regardless the CuO:Cu_2O content. This homogeneity in the shape and size of the nanoparticles makes them ideal to compare how their magnetic response changes as the Cu_2O content increases

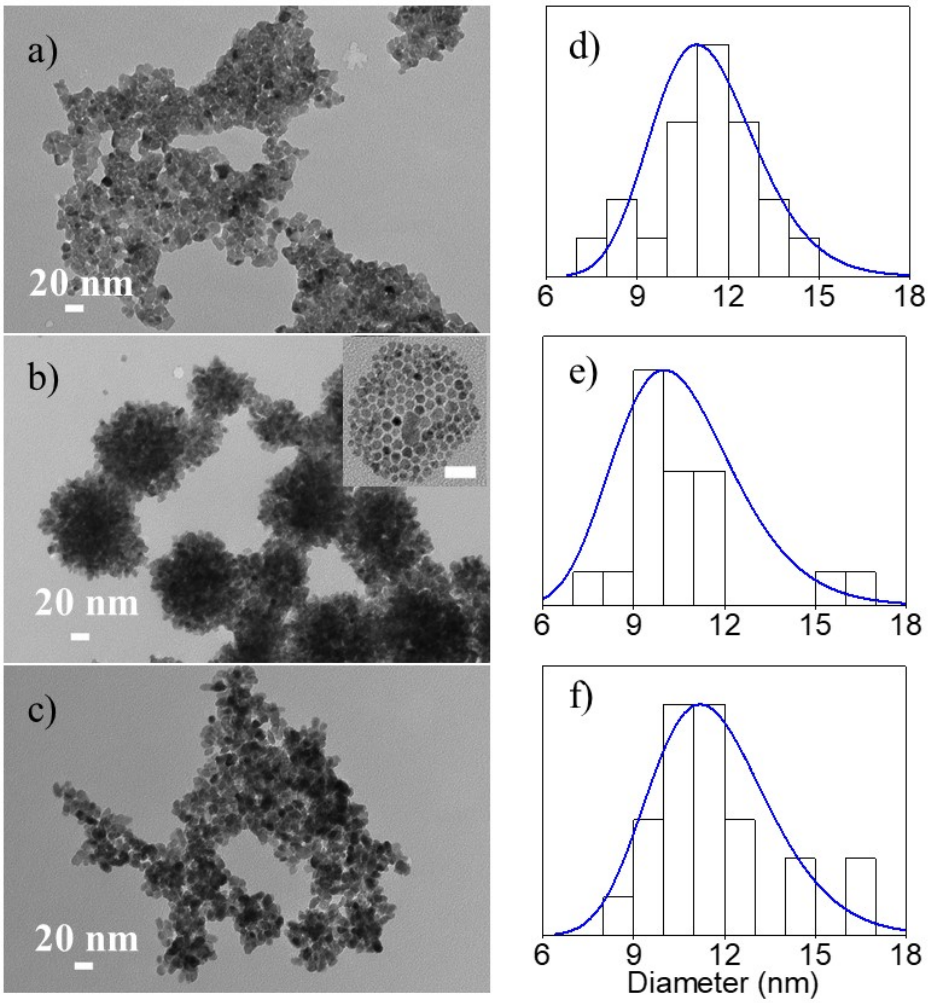

Figure 2. TEM images of a) S1, b) S2, and c) S3 nanocomposites. The individual nanoparticles are very agglomerated. In the inset, a magnification of these nanoparticles is showcased (scale bar is 20 nm). The size distribution histograms are presented in d) S1, e) S2, and f) S3. Fittings to Log-Normal distributions are also included.

Once the samples have been structurally and morphologically characterized, their magnetic response has been studied. First, sample S1, formed by single phase CuO nanoparticles, has been analyzed. The magnetization vs. temperature curves, *M* vs. *T*, under zero-field-cooling/field-cooling (ZFC/FC) conditions are presented in **Figure 3a.** In these *M* vs. *T* curves measured for sample S1, two differentiated temperature ranges can be observed: (i) above 40-50 K, the ZFC/FC

magnetization curves increase with increasing temperature and overlap above 350 K; and (ii) below 50 K, there is a change in the magnetic behavior and the ZFC/FC curves tend to increase as the temperature decreases. This low *T* behavior deviates from the one typically reported for bulk CuO [19,36], for which the *M* vs. *T* curves tend to flatten at low temperatures. In the same way, for bulk CuO, the ZFC/FC curves also tend to increase with increasing *T*, but a clear change is typically observed in the slope of these curves around T_N~230 K, which is not observed in these CuO nanoparticles (S1). This change in the magnetic behavior, between bulk and nanoparticle, is similar to the one reported in other CuO nanoparticle systems [8]. In addition, the appearance of a low temperature upturn in the *M* vs. *T* curves, below 50 K, suggests the existence of an additional magnetic phase, apart from the antiferromagnetic CuO. This additional magnetic phase at low temperatures has been typically associated to the presence of uncompensated surface magnetic moments and/or to other small size effects which are linked to the disruption of the lattice periodicity [7,8,23]. Along these lines, the absence of any change in the slope of the ZFC/FC curves around T_N~230 K suggests that the Néel temperature of these pure CuO nanoparticles is being reduced with respect to the bulk. A reduction of the Néel temperature has also been reported for other CuO nanoparticles, and it has been typically explained in terms of the expansion of the CuO lattice with decreasing particle size [7]. Although, according to XRD analysis, no lattice expansion is observed in sample S1, the existence of a non-negligible lattice strain, as shown before (η = 0.15%), could be affecting the antiferromagnetic (AF) interactions inside the CuO nanoparticles, thereby giving rise to a reduction of the value of T_N.

In the very low temperature region, around 20 K, a cusp in the ZFC curve is observed (indicated by a red arrow in **Figure 3a)**. A similar low temperature cusp has been reported in other antiferromagnetic nanoparticles, and it has been typically attributed to the freezing of the surface

atoms into a spin glass-like phase at very low temperatures [4]. To check if a spin glass-like phase is also being formed at low temperatures in these CuO nanoparticles (sample S1), the *M* vs. *T* measurements have been repeated at higher fields, *H* = 500 Oe. As it is well-known, spin glass phases are very unstable and tend to disappear at high fields [37]. However, as shown in **Figure 3a**, after increasing the field to 500 Oe, the cusp in the *M* vs. *T* curves is still clearly present and does not exhibit any appreciable changes due to the field increases. Hence, this rules out the possibility of the low *T* cusp being related to the formation of a spin glass-like phase. In order to try to shed some light onto this issue, we have plotted the curve obtained by subtracting the FC and ZFC magnetization curves, M_{FC}-M_{ZFC}, as represented in **Figure 3b.** Small changes and deviations in the thermal dependence of the magnetization can be more easily discerned in these M_{FC}-M_{ZFC} measurements. As depicted, the M_{FC}-M_{ZFC} curves present a clear change in the slope below 20 K, thereby supporting the presence of 2 different magnetic regimes, above and below this temperature, as was mentioned before. Besides, as it happened with the ZFC/FC curves, the position of this steep rise does not change when increasing the field from 100 to 500 Oe. A similar sharp change in the M_{FC}-M_{ZFC} curves was also reported by Punnose *et al* [7] for 6.6 nm CuO nanoparticles at temperature values below 40 K. They related this rise in their M_{FC}-M_{ZFC} curves to a reduction of the Neel temperature, down to T_N = 40 K. This decrease of T_N was associated to the modification of the AF interactions between the Cu^{2+} magnetic moments within the core, due to the lattice expansion they observed in their nanoparticles. However, in sample S1, no appreciable lattice modification was observed by XRD. On the other hand, Batsaikhan *et al* [23] also reported a similar upturn in the spontaneous magnetization of CuO nanoparticles below 10 K. In their case, they related this upturn to a change in the main magnetic contributors as the temperature decreased: the core magnetic moments above the upturn, and the surface magnetic

moments below it. Therefore, the presence of an upturn in M_{FC}-M_{ZFC} curves for sample S1 around 20 K could also be indicating a similar change in the magnetic contributors. To gain further insight about this, the isothermal *M* vs. *H* curves of S1 nanoparticles have been measured at different temperatures: 2, 5, and 300 K (**Figure 3c**). The presence of two magnetic components is clearly noticeable, with a high field slope above ~1.5 kOe and a hysteretic behavior below that field.

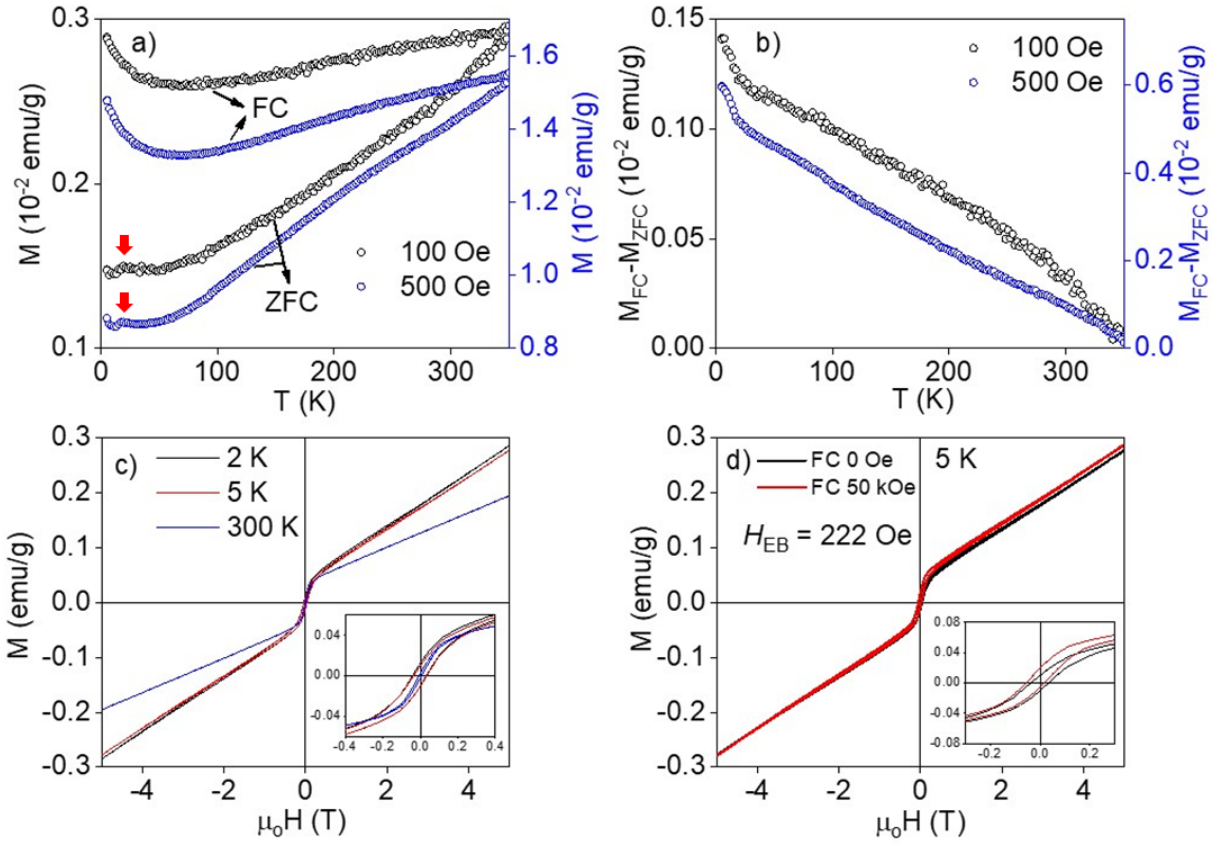

Figure 3. Magnetic measurements for S1 nanocomposites (pure CuO). a) Magnetization vs. temperature curves for CuO nanoparticles, measured under ZFC and FC conditions at an applied field of 100 and 500 Oe. The red arrows indicate the position of a low temperature cusp in the ZFC curves. b) Subtraction of the ZFC and FC magnetization curves, M_{FC}-M_{ZFC}. c) Hysteresis loops measured at 2, 5, 300 K. d) Hysteresis loops measured at 5 K under ZFC and FC (50 kOe) conditions.

Table II. Coercive field (H_C), high-field susceptibility (χ), and extrapolated saturation magnetization (M_0) at 5 and 300 K

Sample	H_C at 5 K (Oe)	H_C at 300 K (Oe)	χ at 5 K (10^{-6} emu·g^{-1}·Oe^{-1})	χ at 300 K (10^{-6} emu·g^{-1}·Oe^{-1})	M_0 at 5 K (emu/g)	M_0 at 300 K (emu/g)
S1	338	65	4.75	3.14	0.041	0.038
S2	430	~0	5.10	2.32	0.005	~0
S3	485	~0	1.46	0.11	0.002	~0

We have first focused on the high field region of these *M* vs. *H* curves. At 300 K, this high field slope could be associated in principle to the typical expected paramagnetism of CuO above T_N. However, as indicated in **Table II**, the obtained high-field susceptibility value, $\chi = 3.14\ 10^{-6}$ emu·g^{-1}·Oe^{-1} (being $M = \chi H$), is appreciably higher than the values typically reported for bulk CuO ($\chi = 0.6\ 10^{-6}$ emu·g^{-1}·Oe^{-1} , see for example [23]). This difference becomes even more noticeable at low temperatures (2 and 5 K), where the high-field antiferromagnetic susceptibility reaches an even higher value, $\chi = 4.75\ 10^{-6}$ emu·g^{-1}·Oe^{-1}. Therefore, these results clearly indicate an enhancement of the antiferromagnetic response in CuO nanoparticles (sample S1) compared to bulk.

On the other hand, in the low field regime, *M* increases rapidly with increasing field, up to ~1.5 kOe, describing a clear hysteresis not observed in bulk CuO. This hysteresis persists in the whole range of temperatures analyzed, even at 300 K, and it has been typically related in the literature to the existence of a "weak ferromagnetic" contribution in CuO nanoparticles [7,23–25]. The saturation magnetization of this ferromagnetic contribution, M_0, obtained after subtracting the high-field slope from the *M* vs. *H* curves, reaches a value of 0.041 emu/g at 5 K. This value is similar to those reported for other CuO nanoparticles such as 8.8 nm CuO nanoparticles, with a saturation of 0.04 emu/g at 1.8 K [8]. However, these saturation values are much higher (> 150 times) than

those typically reported for bulk CuO samples (0.00025 emu/g) [23], indicating a large enhancement of the FM contribution for CuO nanoparticles compared to bulk.

These enhancements of both AF and FM contributions in these 11 nm CuO nanoparticles cannot be simply attributed to the existence of uncompensated surface Cu^{2+} magnetic moments [7], nor to the appearance of surface oxygen vacancies or defects [25], since, on the one hand, the number of surface atoms is relatively small (~ 20% of the atoms on the surface), and, on the other hand, XRD results for sample S1 revealed a high crystallinity with lattice parameters comparable to bulk. To this respect, recently, Batsaikhan *et al* [23] revealed a similar large increase in the FM and AF contributions of CuO nanoparticles compared to bulk. By using a combination of magnetization and neutron diffraction measurements, they indicated that these changes were mainly caused by a charge redistribution in the whole nanoparticle, which was triggered by the disruption of the lattice at the surface (the so called "small size effects"). This gave rise to an enhancement of the magnetic coupling between Cu ions (especially relevant for the magnetic moments on the surface), thereby increasing the FM (surface) and AF (core) contributions [23]. A similar effect could also be taking place in sample S1. Moreover, the presence of strong FM interactions for the surface atoms could also explain the absence of a spin glass behavior at low temperatures for sample S1, as was mentioned before in the analysis of the *M* vs *T* curves.

To further investigate this, the coupling between the core (AF) and surface (FM) atoms has been probed by studying the possible presence of exchange bias (EB) at low temperatures in these nanoparticles [7]. As shown in **Figure 3d**, the hysteresis loop measured after field-cooling (FC) sample S1 while applying a field of 50 kOe exhibits a shift towards negative fields at 5 K, which is a clear fingerprint for EB. The value of the exchange bias field, H_{EB}, at 5 K is ~220 Oe, slightly below the one reported for other similar CuO nanoparticles [7]. However, it should be noted that,

unlike what happened in these previous reports on CuO nanoparticles, no broadening of the FC hysteresis loop (increase in coercivity) was observed. An increase in coercivity, H_C, for the FC hysteresis loops measured at low temperatures has been typically associated with a FM and AF coupling between the core and the surface atoms [24]. Therefore, the presence of EB but without an increase in H_C for sample S1 suggests only a weak interfacial coupling between FM (surface) and AF (core) components in S1 nanoparticles.

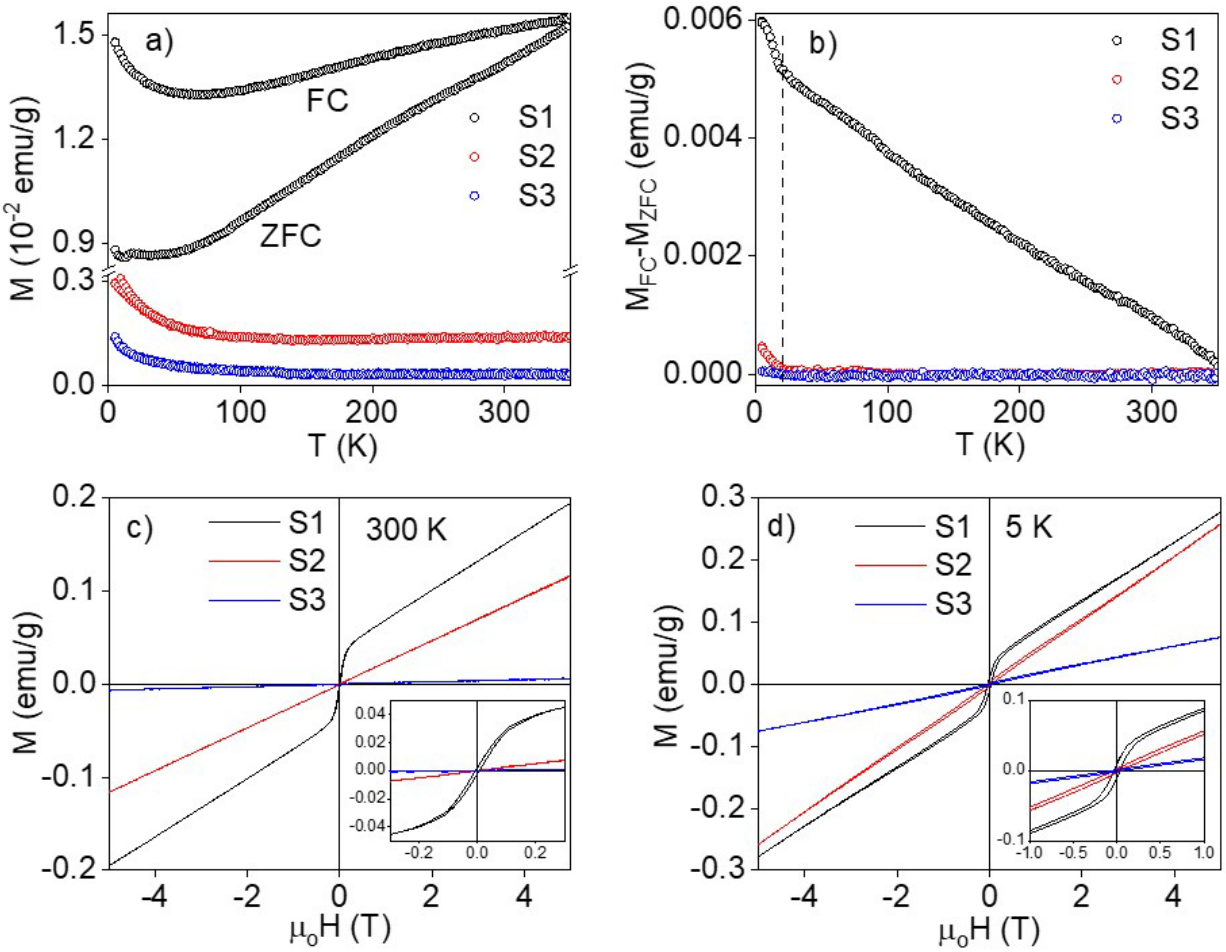

Figure 4. Comparison of the magnetic measurements for S1, S2, and S3 nanocomposites. a) Temperature variation of magnetization in ZFC and FC conditions at an applied field of 500 Oe. b) Thermal variation of difference magnetization [M_{FC}-M_{ZFC}]. c) Hysteresis loops measured at 300 K. d) Hysteresis loops measured after ZFC at 5 K.

Once an overall idea of the magnetic response of the single phase CuO nanoparticles has been obtained, the magnetic behavior of the CuO/Cu_2O nanocomposites has been studied (samples S2 and S3). As mentioned before, although bulk Cu_2O is diamagnetic, in nanoparticle form, a paramagnetic behavior has been frequently reported. This has been frequently associated to the presence of Cu^{2+} ions on the surface of the Cu_2O nanoparticles, due to oxygen excess and/or surface defects [38,39]. To better understand the effect of Cu_2O in the magnetic response of CuO/Cu_2O nanocomposites, the ZFC/FC curves of CuO nanoparticles (S1) and CuO/Cu_2O nanocomposites (S2 and S3) have been compared in **Figure 4a**. As depicted, the ZFC and FC magnetization curves of samples S2 and S3 remain nearly constant down to 15-20 K, contrary to what is observed for sample S1. Moreover, the ZFC/FC curves for S2 and S3 present an upturn below 15 K, in a similar way to S1, but without any noticeable cusp this time. In addition, the increase of the Cu_2O content leads to a decrease of the net magnetization value for S2 and S3 compared to S1. All these results indicate a suppression of both FM and AF phases in S2 and S3. **Figure 4b** depicts the M_{FC}-M_{ZFC} curves for these three samples. As the Cu_2O content is increased, the steep rise below 20 K, which was observed for sample S1, greatly diminishes for sample S2 (34% of Cu_2O), and nearly completely disappears for sample S3 (91% Cu_2O content). This would indicate that in sample S2, both FM and AF components are still present, albeit weakened if compared to sample S1, but they are largely suppressed for sample S3, due to the large increase in Cu_2O amount.

Figure 4c presents the hysteresis loops, *M* vs. *H*, measured at 300 K for the three samples. The corresponding H_C, M_0, and χ values are indicated in **Table II**. Whereas sample S1 shows a clear hysteresis and coercivity in the whole range of temperatures, as was discussed before, samples S2 and S3 no longer exhibit any hysteresis at room temperature. In addition, the high-field

susceptibility tends to decrease with increasing Cu_2O content, being this reduction especially noticeable for sample S3. As indicated in **Table II,** at 300 K the high-field susceptibility decreases from $\chi = 3.14\ 10^{-6}$ emu·g^{-1}·Oe^{-1} for sample S1, to $\chi = 2.32\ 10^{-6}$ emu·g^{-1}·Oe^{-1} (~26 % decrease) for S2, and to $\chi = 0.11\ 10^{-6}$ emu·g^{-1}·Oe^{-1} (~96 % decrease) for S3. As can be seen, these percentage decrease numbers are comparable to the increase in Cu_2O content, 34% for S2 and 91 % for S3. This indicates that, at room temperature, the increase in Cu_2O content (diamagnetic) is progressively suppressing the AF order associated to CuO. A different effect is obtained, however, at low temperatures (5 K), as depicted in **Figure 4d**. Here it is interesting to notice that in the case of sample S2, the high-field slope obtained at 5 K, $\chi = 5.10\ 10^{-6}$ emu·g^{-1}·Oe^{-1}, is even higher than the one obtained for sample S1, $\chi = 4.75\ 10^{-6}$ emu·g^{-1}·Oe^{-1}. This means that, at low temperature, the 34% Cu_2O phase inside the nanocomposite is giving an additional contribution to the high-field slope, apart from the AF contribution from CuO. However, for sample S3, with 91% Cu_2O phase, the high-field slope obtained at 5 K is $\chi = 1.46\ 10^{-6}$ emu·g^{-1}·Oe^{-1}, a lower value than the one obtained for S1 and S2, but still very different from the negative χ value typically reported in bulk diamagnetic Cu_2O at 5 K (e.g. $\chi = -\ 9.5\ 10^{-6}$ emu·g^{-1}·Oe^{-1} [40]). On the other hand, in the lower field region of the *M* vs. *H* curves, the hysteresis observed for samples S2 and S3 at 5 K presents a nearly null saturation value and is clearly different from the one obtained for sample S1 (see **Table II**). Coercivity values of 338, 430 and 485 Oe are obtained for S1, S2, and S3, respectively, at 5 K.

Therefore, these results are indicating a surprising effect of Cu_2O phase inside the nanocomposite. On the one hand, even at relatively low contents, the Cu_2O is strongly suppressing the FM order previously described for pure CuO nanoparticles, in the whole range of temperatures. As mentioned before, Gao *et al.* [32,33] reported in both bulk and micron sized CuO/Cu_2O particles

an increase of the ferromagnetic order with increasing Cu_2O amount, till a point after which the FM order rapidly decreased. They attributed the FM enhancement to an interface coupling effect between the CuO and Cu_2O phases. However, in the CuO/Cu_2O nanocomposites studied in this work, no such enhancement of the FM order has been observed. Instead, an enhancement of the AF contribution at low temperatures has been observed for 34 % Cu_2O (sample S2), which is no longer present for 91 % Cu_2O (sample S3). This enhancement of the AF contribution for S2 cannot be explained just by adding the PM contribution of Cu_2O with the AF contribution of CuO, as observed in Table II. Therefore, it is probably related to an interface effect between CuO and Cu_2O phases inside the nanocomposites. This is supported by the increase in coercivity observed for sample S2 at 5 K compared to sample S1. For sample S3, the low CuO content (9%), together with the lattice deformation reported in the XRD results, is effectively suppressing both the FM and AF order of CuO. Despite this, there is some extra magnetic order at low temperatures (as denoted by the remanent high-field slope and the increase in coercivity at 5 K). This suggests again the presence of interface effects between CuO/Cu_2O, although less pronounced than in the case of sample S2.

Conclusions

In this work 11-12 nm single phase CuO nanoparticles and CuO/Cu_2O nanocomposite with varying phase ratio have been successfully synthesized using a solvothermal process. It was found that the CuO/Cu_2O nanocomposite phase ratio could be effectively controlled by varying the solvothermal reaction temperature, while the morphology and size of the nanoparticles remained nearly constant. This has facilitated the comparison between the three samples. Rietveld refinements show a progressive unit cell expansion of CuO phase in CuO/Cu_2O nanocomposites compared to

pure CuO nanoparticles. Room temperature FM is observed only in single phase CuO nanoparticles. Magnetic measurements indicate that the FM and AF contributions are appreciably enhanced in CuO nanoparticles, compared to bulk, but as the amount of Cu_2O increases, the FM contribution is heavily suppressed in the whole range of temperatures. On the other hand, at low temperatures the AF contribution first increased (for 34 % of Cu_2O) and then decreased (for 91 % of Cu_2O) with increasing Cu_2O content. This has been associated to the presence of additional interface effects between the CuO and Cu_2O phases. These results differ from those reported in other CuO/Cu_2O composites, both in bulk and microparticle shape, and they clearly indicate that at the nanoscale, additional interface and surface contributions come into play giving rise to unexpected magnetic phenomena, such as the increase of the AF susceptibility observed for sample S2 at 5 K compared to S1. Therefore, the results obtained in this work stress the importance of carefully tuning the CuO/Cu_2O content at the nanoscale. In this regard, the observed suppression of the FM order and enhancement of the AF order in CuO/Cu_2O nanocomposites can pave the way to a new and novel breed of magnetic materials of emergent device interest.

Acknowledgements

The work was supported by the Vietnam National Foundation for Science and Technology Development (NAFOSTED) under Grant number 103.02-2019.314. J.A. and L.F.B acknowledge financial support provided through the Spanish "Ministerio de Ciencia, Investigación y Universidades" projects: MAT2017-83631-C3-R and PID2020-115704RB-C3. E.M.J. acknowledges “Beca Concepción Arenal” BDNS: 406333 granted by the Gobierno de Cantabria and the Universidad de Cantabria. R.D. acknowledges Manh-Huong Phan and Hariharan Srikanth

for synthesis and characterization facilities in Functional Materials Laboratory, Department of Physics, University of South Florida, Tampa, Florida, 33620, United States.

References

[1] B.T. Matthias, R.M. Bozorth, J.H. Van Vleck, Ferromagnetic Interaction in EuO, Phys. Rev. Lett. 7 (1961) 160. https://doi.org/10.1103/PhysRevLett.7.160.

[2] D.E. Speliotis, Magnetic recording beyond the first 100 Years, J. Magn. Magn. Mater. 193 (1999) 29–35. https://doi.org/10.1016/S0304-8853(98)00399-0.

[3] A. Sundaresan, R. Bhargavi, N. Rangarajan, U. Siddesh, C.N.R. Rao, Ferromagnetism as a universal feature of nanoparticles of the otherwise nonmagnetic oxides, Phys. Rev. B. 74 (2006) 161306. https://doi.org/10.1103/PhysRevB.74.161306.

[4] N. Rinaldi-Montes, P. Gorria, D. Martínez-Blanco, A.B. Fuertes, L. Fernández Barquín, J. Rodríguez Fernández, I. De Pedro, M.L. Fdez-Gubieda, J. Alonso, L. Olivi, G. Aquilanti, J.A. Blanco, Interplay between microstructure and magnetism in NiO nanoparticles: breakdown of the antiferromagnetic order, Nanoscale. 6 (2013) 457–465. https://doi.org/10.1039/C3NR03961G.

[5] C. Echevarria-Bonet, D.P. Rojas, J.I. Espeso, J. Rodríguez Fernández, L. Rodríguez Fernández, P. Gorria, J.A. Blanco, M.L. Fdez-Gubieda, E. Bauer, G. André, L. Fernández Barquín, Size-induced superantiferromagnetism with reentrant spin-glass behavior in metallic nanoparticles of TbCu2, Phys. Rev. B - Condens. Matter Mater. Phys. 87 (2013) 180407. https://doi.org/10.1103/PhysRevB.87.180407.

[6] N. Rinaldi-Montes, P. Gorria, A.B. Fuertes, D. Martínez-Blanco, Z. Amghouz, I. Puente-Orench, L. Olivi, J. Herrero-Martín, M.P. Fernandez-Garcia, J. Alonso, M.H. Phan, H. Srikanth, X. Marti, J.A. Blanco, Entangled core/shell magnetic structure driven by surface magnetic symmetry-breaking in Cr2O3 nanoparticles, J. Mater. Chem. C. 10 (2022) 1798–1807. https://doi.org/10.1039/d1tc04947j.

[7] A. Punnoose, H. Magnone, M.S. Seehra, J. Bonevich, Bulk to nanoscale magnetism and exchange bias in CuO nanoparticles, Phys. Rev. B. 64 (2001) 174420. https://doi.org/10.1103/PhysRevB.64.174420.

[8] H.M. Xiao, L.P. Zhu, X.M. Liu, S.Y. Fu, Anomalous ferromagnetic behavior of CuO nanorods synthesized via hydrothermal method, Solid State Commun. 141 (2007) 431–435. https://doi.org/10.1016/J.SSC.2006.12.005.

[9] V. Bisht, K.P. Rajeev, S. Banerjee, Anomalous magnetic behavior of CuO nanoparticles, Solid State Commun. 150 (2010) 884–887. https://doi.org/10.1016/J.SSC.2010.01.048.

[10] R. Wick, S.D. Tilley, Photovoltaic and Photoelectrochemical Solar Energy Conversion with Cu2O, J. Phys. Chem. C. 119 (2015) 26243–26257.

https://doi.org/10.1021/ACS.JPCC.5B08397.

[11] J.H. Bang, A. Mirzaei, M.S. Choi, S. Han, H.Y. Lee, S.S. Kim, H.W. Kim, Decoration of multi-walled carbon nanotubes with CuO/Cu2O nanoparticles for selective sensing of H2S gas, Sensors Actuators B Chem. 344 (2021) 130176. https://doi.org/10.1016/J.SNB.2021.130176.

[12] J. Singh, S. Juneja, R.K. Soni, J. Bhattacharya, Sunlight mediated enhanced photocatalytic activity of TiO2 nanoparticles functionalized CuO-Cu2O nanorods for removal of methylene blue and oxytetracycline hydrochloride, J. Colloid Interface Sci. 590 (2021) 60–71. https://doi.org/10.1016/J.JCIS.2021.01.022.

[13] N. Kumar, S.S. Parui, S. Limbu, D.K. Mahato, N. Tiwari, R.N. Chauhan, Structural and optical properties of sol–gel derived CuO and Cu2O nanoparticles, Mater. Today Proc. 41 (2021) 237–241. https://doi.org/10.1016/J.MATPR.2020.08.800.

[14] A.M. Ghadiri, N. Rabiee, M. Bagherzadeh, M. Kiani, Y. Fatahi, A. Di Bartolomeo, R. Dinarvand, T.J. Webster, Green synthesis of CuO- and Cu2O-NPs in assistance with high-gravity: The flowering of nanobiotechnology, Nanotechnology. 31 (2020) 425101. https://doi.org/10.1088/1361-6528/ABA142.

[15] J. Albo, M.I. Qadir, M. Samperi, J.A. Fernandes, I. de Pedro, J. Dupont, Use of an optofluidic microreactor and Cu nanoparticles synthesized in ionic liquid and embedded in TiO2 for an efficient photoreduction of CO2 to methanol, Chem. Eng. J. 404 (2021) 126643. https://doi.org/10.1016/J.CEJ.2020.126643.

[16] B.X. Yang, J.M. Tranquada, G. Shirane, Neutron scattering studies of the magnetic structure of cupric oxide, Phys. Rev. B. 38 (1988) 174. https://doi.org/10.1103/PhysRevB.38.174.

[17] S.B. Ota, E. Gmelin, Incommensurate antiferromagnetism in copper (II) oxide: Specific-heat study in a magnetic field, Phys. Rev. B. 46 (1992) 11632. https://doi.org/10.1103/PhysRevB.46.11632.

[18] A. Junod, D. Eckert, G. Triscone, J. Muller, W. Reichardt, A study of the magnetic transitions in CuO: specific heat (1-330 K), magnetic susceptibility and phonon density of states, J. Phys. Condens. Matter. 1 (1989) 8021. https://doi.org/10.1088/0953-8984/1/43/004.

[19] M. O'keeffe, F.S. Stone, The magnetic susceptibility of cupric oxide, J. Phys. Chem. Solids. 23 (1962) 261–266. https://doi.org/10.1016/0022-3697(62)90010-0.

[20] M.S. Seehra, Z. Feng, R. Gopalakrishnan, Magnetic phase transitions in cupric oxide, J. Phys. C Solid State Phys. 21 (1988) L1051–L1054. https://doi.org/10.1088/0022-3719/21/30/009.

[21] D.D. Lawrie, J.P. Franck, C.T. Lin, Search for an isotope effect in the antiferromagnetic transitions of cupric oxide CuO, Phys. C Supercond. Its Appl. 297 (1998) 59–63. https://doi.org/10.1016/S0921-4534(97)01846-7.

[22] J.W. Loram, K.A. Mirza, C.P. Joyce, A.J. Osborne, Specific-Heat Evidence for Quasi-1D Magnetic Order in CuO, Europhys. Lett. 8 (1989) 263. https://doi.org/10.1209/0295-

5075/8/3/010.

[23] E. Batsaikhan, C.H. Lee, H. Hsu, C.M. Wu, J.C. Peng, M.H. Ma, S. Deleg, W.H. Li, Largely Enhanced Ferromagnetism in Bare CuO Nanoparticles by a Small Size Effect, ACS Omega. 5 (2020) 3849–3856. https://doi.org/10.1021/acsomega.9b02913.

[24] M.S. Seehra, A. Punnoose, Particle size dependence of exchange-bias and coercivity in CuO nanoparticles, Solid State Commun. 128 (2003) 299–302. https://doi.org/10.1016/J.SSC.2003.08.029.

[25] H. Qin, Z. Zhang, X. Liu, Y. Zhang, J. Hu, Room-temperature ferromagnetism in CuO sol–gel powders and films, J. Magn. Magn. Mater. 322 (2010) 1994–1998. https://doi.org/10.1016/J.JMMM.2010.01.021.

[26] D. Gao, Z. Yang, J. Zhang, G. Yang, Z. Zhu, J. Qi, M. Si, D. Xue, Transforming from paramagnetism to room temperature ferromagnetism in CuO by ball milling, AIP Adv. 1 (2011) 042168. https://doi.org/10.1063/1.3670360.

[27] K. Karthik, N. Victor Jaya, M. Kanagaraj, S. Arumugam, Temperature-dependent magnetic anomalies of CuO nanoparticles, Solid State Commun. 151 (2011) 564–568. https://doi.org/10.1016/J.SSC.2011.01.008.

[28] D. Gao, G. Yang, J. Li, J. Zhang, J. Zhang, D. Xue, Room-temperature ferromagnetism of flowerlike CuO nanostructures, J. Phys. Chem. C. 114 (2010) 18347–18351. https://doi.org/10.1021/jp106015t.

[29] R.S. Bhalerao-Panajkar, M.M. Shirolkar, R. Das, T. Maity, P. Poddar, S.K. Kulkarni, Investigations of magnetic and dielectric properties of cupric oxide nanoparticles, Solid State Commun. 151 (2011) 55–60. https://doi.org/10.1016/j.ssc.2010.10.024.

[30] I.S. Brandt, M.A. Tumelero, E. Lima, D.L. da Silva, R.D. Zysler, R. Faccio, A.A. Pasa, Enhanced defect-mediated ferromagnetism in Cu2O by Co doping, J. Magn. Magn. Mater. 441 (2017) 374–386. https://doi.org/10.1016/j.jmmm.2017.05.057.

[31] A. Ahmed, N.S. Gajbhiye, Room temperature ferromagnetism in Mn, Ni and Co ions doped Cu2O nanorods, J. Solid State Chem. 183 (2010) 3100–3104. https://doi.org/10.1016/j.jssc.2010.09.040.

[32] D. Gao, Z. Zhang, Q. Xu, J. Zhang, Z. Yan, J. Yao, D. Xue, Room temperature ferromagnetism in CuO/Cu2O microspheres: Towards interface effect, Appl. Phys. Lett. 104 (2014) 022406. https://doi.org/10.1063/1.4861884.

[33] D. Gao, Z. Zhang, Z. Yang, D. Xue, Interface mediated ferromagnetism in bulk CuO/Cu2O composites, Appl. Phys. Lett. 101 (2012) 132416. https://doi.org/10.1063/1.4755766.

[34] P. (Pierre) Villars, L.D. (Lauriston D.. Calvert, W.B. (William B. Pearson, Pearson's handbook of crystallographic data for intermetallic phases, American Society for Metals, 1985.

[35] M.L. Foo, Q. Huang, J.W. Lynn, W.L. Lee, T. Klimczuk, I.S. Hagemann, N.P. Ong, R.J. Cava, Synthesis, structure and physical properties of Ru ferrites: BaMRu 5O11 (M=Li and

Cu) and BaM′2Ru 4O11 (M′=Mn, Fe and Co), J. Solid State Chem. 179 (2006) 563–572. https://doi.org/10.1016/j.jssc.2005.11.014.

[36] D.M. Chethana, T.C. Thanuja, H.M. Mahesh, M.S. Kiruba, A.S. Jose, H.C. Barshilia, J. Manjanna, Synthesis, structural, magnetic and NO2 gas sensing property of CuO nanoparticles, Ceram. Int. 47 (2021) 10381–10387. https://doi.org/10.1016/J.CERAMINT.2020.06.129.

[37] J.A. Mydosh, Spin Glasses: An Experimental Introduction, Taylor and Francis London, CRC Press, 1993. https://doi.org/10.1201/9781482295191.

[38] M.B. Mahajan, M.S. Pavan, P.A. Joy, Ferromagnetic properties of glucose coated Cu2O nanoparticles, Solid State Commun. 149 (2009) 2199–2201. https://doi.org/10.1016/j.ssc.2009.09.013.

[39] P.H. Shih, J.Y. Ji, Y.R. Ma, S.Y. Wu, Size effect of surface magnetic anisotropy in Cu2 O nanoparticles, J. Appl. Phys. 103 (2008) 07B735. https://doi.org/10.1063/1.2839331.

[40] C. Chen, L. He, L. Lai, H. Zhang, J. Lu, L. Guo, Y. Li, Magnetic properties of undopedCu2O fine powders with magnetic impurities and/or cation vacancies, J. Phys. Condens. Matter. 21 (2009) 145601. https://doi.org/10.1088/0953-8984/21/14/145601.